Pyrolysis of mixed plastic fractions – Development of predictive models for yield and oil quality

Henneberg, Rasmus Uglebjerg; Nielsen, Rudi P.; Simonsen, Morten Enggrob

Published in:
Journal of Analytical and Applied Pyrolysis

DOI (link to publication from Publisher):
10.1016/j.jaap.2023.106037

Publication date:
2023

Document Version
Publisher's PDF, also known as Version of record

Citation for published version (APA):
Henneberg, R. U., Nielsen, R. P., & Simonsen, M. E. (2023). Pyrolysis of mixed plastic fractions – Development of predictive models for yield and oil quality. *Journal of Analytical and Applied Pyrolysis*, *173*, Article 106037. https://doi.org/10.1016/j.jaap.2023.106037

Journal of Analytical and Applied Pyrolysis 173 (2023) 106037

Contents lists available at ScienceDirect

Journal of Analytical and Applied Pyrolysis

journal homepage: www.elsevier.com/locate/jaap

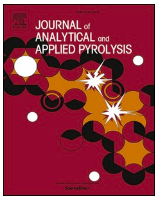

Pyrolysis of mixed plastic fractions – Development of predictive models for yield and oil quality

Rasmus Uglebjerg Henneberg, Rudi Pankratz Nielsen, Morten Enggrob Simonsen [*]

Department of Chemistry and Bioscience, Aalborg University, Niels Bohrs Vej 8, 6700, Esbjerg, Denmark

ARTICLE INFO

Keywords:
Pyrolysis
Modeling
Mixed plastics
Oil production

ABSTRACT

Pyrolysis of plastic mixtures has shown to form complex mixtures of oil, which is difficult to predict. Interaction effects between plastics have shown to affect both the oil composition and the yield distribution of oil, char, and gas. This work aims to generate models for the prediction of oil and char yield, acid number, and viscosity based on the feed composition. Besides the oil composition based on the reactor feed was mapped. Pyrolysis was performed in a batch reactor with a mixture of PP, PE, EVA, PET, PS and PA, where the content of PET, PS and PA were varied from 0% to 15%. The developed models showed a decrease in oil yield of 10% when 15% PS was interchanged with PET. Char content, acid number, and viscosity were shown to increase with the content of PET and lowered with the content of PS. PA caused an increase in char yield and viscosity, while it did not affect the acid number. The models R^2-values varied from 0.87 to 0.96, showing that most of the variation in the responses can be explained by the differences in feed composition. The oil composition was found to mainly consist of hydrocarbons (C10 +), naphta and aromatics with only a small precense of alcohol and acid. The content of aromatic hydrocarbons is increased by the presence of PS, due to formation of styrene and toluene while the acid content increases with the PET content.

1. Introduction

Plastic recycling has become a highly relevant topic, with 367 million tons of plastic produced in 2020 [1]. In 2018, Europe collected 29.1 million tons of plastic as post-consumer waste, of which 32.5% was recycled, 42.6% was energy recovered, and 24.9% was landfilled [2]. The most commonly used recycling technique is mechanical recycling, which recycles more than 5 million tons of plastic per year in Europe [3,4]. However, mechanical recycling has several issues, as it produces products with diminished mechanical properties and is unable to handle mixed plastics due to the immiscibility of the plastics [5,6].

Post-consumer waste (PCW) consists mostly of packaging materials, with the main polymers being polypropylene (PP), polyethylene terephthalate (PET), polyethylene (PE), and polystyrene (PS) [2,7]. PCW is made up of various types of packaging, such as bottles, trays, and films, with multilayered plastic films being the most troublesome fraction. These films contain several different plastic types, including PE, PP, PET, PS, polyamide (PA), and ethylene-vinyl acetate (EVA) [8], which are difficult or impossible to separate and therefore cannot be recycled mechanically [8]. Additionally, PCW plastics are often contaminated by organics [2,8], which creates another barrier for mechanical recycling. As a result, alternative recycling methods are needed to handle PCW, such as chemical recycling by pyrolysis [9,10].

Pyrolysis of plastics produces oil, gas, char, and wax, all of which can be used to create new materials [4,7]. The ratio and composition of these products are influenced by various factors, such as temperature, pressure, residence time, carrier gas, and feedstock. The effect of temperature depends on the type of plastic being pyrolyzed [7]. In general, temperatures of 500 °C or higher increase gas output, while temperatures between 300 °C and 500 °C are used if oil is the desired product. Higher pressures have been shown to decrease the molecular chain size, resulting in increased gas production, while residence time is only a factor at temperatures below 450 °C [7,11]. Purging with nitrogen before pyrolysis has been found to increase the oil yield from 33.8% to 92.3% [12]. Nitrogen is the most commonly used purge gas due to its low toxicity, flammability, and cost compared to other gases tested [7].

Several studies have investigated the fractions formed during pyrolysis using single-feed plastics, and the results are reported in Table 1. The wax and oil fractions are combined into a single category due to both phases being condensed after pyrolysis.

---

[*] Corresponding author.
E-mail address: mes@bio.aau.dk (M.E. Simonsen).

https://doi.org/10.1016/j.jaap.2023.106037
Received 23 December 2022; Received in revised form 27 May 2023; Accepted 3 June 2023

Table 1
Yield of pyrolysis of single plastics by plastic type [7,13–19] * Optimal temperature for oil yield.

Polymer type	Oil Yield (wt%)	Gas yield (wt%)	Char yield (wt %)	Optimal temperature* (°C)	Source
PET	23–45	52–77	6–17	500	[7,13]
LDPE	85–95	5–15	-	500	[7,14]
PP	70–86	6–14	0–13	500	[13,15, 16]
PS	93–97	-	-	450	[17]
PA6	86	13	1	475	[19]
EVA	90	-	10	-	[18]

PET gives low oil yields due to the presence of oxygen, leading to the formation of CO, CO_2, and char [7,13]. LDPE produces large amounts of oil, minimal gas, and insignificant amounts of char [7]. PP produces significant oil yields with minor gas and char formation, making it an ideal feed for pyrolysis as it doesn't form waxes or acids [7]. PS forms mainly oils without waxes, which makes it a suitable feed for pyrolysis [7]. PA produces large oil and minor gas amounts, while EVA forms char and acetic acid, which can corrode equipment [18].

Gas from plastic pyrolysis primarily comprises hydrocarbons such as methane, ethane, and propane, with the presence of oxygen leading to CO and CO_2 formation [20,21]. Pyrolysis of PA results in small amounts of nitrogen compounds such as ammonia and cyanide [21,22].

Where pyrolysis of single type plastics has received much attention over the years, then the pyrolysis of mixed plastics has received far less. This provides a significant obstacle in the chemical recycling of PCW as this fraction will undoubtedly be mixed plastics due to the inability to separate for instance multilayer films. Some studies have been conducted on these mixed plastics and has shown that pyrolysis of mixed plastics leads to unpredictable yields and products due to interactions between the polymers during pyrolysis. Williams et al. pyrolyzed a mixture of HDPE, PP, PS, PVC, and PET, forming 48.7% oil instead of the predicted 72.3% based on the yields from each single plastic pyrolysis, indicating a 23.7% decline in oil yield [20].

The oil phase from pyrolysis contains different products based on the plastics pyrolyzed. PET mainly forms benzoic acid, PP 2,4-dimethyl-1-heptene, PS styrene, PA caprolactam, and EVA acetic acid [23–26]. These are the main products; however, a number of additional products are also formed during pyrolysis, increasing the complexity of the oil composition. Interaction effects between different types of plastics in pyrolysis have been shown to impact both oil yield and composition compared to single type plastics [20].

The aim of this work is to develop statistically based predictive models for the yield of oil and gas, as well as acid value and viscosity, based on the composition of the polymer feedstock and thus providing increased insight into the pyrolysis of mixed plastics such as PCW. The models were created based on experiments performed on polymer mixtures consisting of PP, PE, EVA, PET, PS, and PA. These plastic types were selected because they are all found in multilayered plastic films [8], where the plastic types cannot be separated. The experiments were conducted by varying a portion of the feed composition while keeping the content of remaining components constant using a mixture design. The oils were analyzed to obtain an overview of the variance in oil composition based on the feed composition.

2. Materials and methods

The structure of the experiments was developed using a simplex lattice mixture design, where only part of the reactor feed is varied. Mixture designs are used when the variables cannot be varied independently, but must add up to 100% of the feed. In this case a 2D simplex was used, with each corner representing a pure polymer. The simplex was subsequently covered uniformly by sampling points (experimental feedstock compositions) forming the lattice as illustrated in Fig. 1.

Due to PE and PP being present in most waste plastics and EVA commonly used in multilayer films it was chosen to keep the content of these constant forming a baseline at 10%, 70%, and 5% respectively. The variation was introduced with PET, PS, and PA content which was varied from 0% to 15%. Table 2 provides an overview of the experimental plan using this mixture design and conducting experiments in duplicates.

2.1. Materials

PP, PE, and PET polymers were supplied by FiberVisions, Denmark while EVA and PS were supplied by SigmaAldrich, all as granulates with diameter of 3–5 mm. PA was supplied by OTV Plast as PA6 XT NATUR ø6 (mm) as round bars, which were chopped into 3–5 mm pieces.

2.2. Experimental procedure

The experimental setup is shown in Fig. 2.

Nitrogen (1) was used as the carrier gas and the reactor was a 300 ml BC-1 reactor from High-Pressure Equipment Co. (7). The reactor was heated by a hot plate (8) and a heating mantle controlled (6) by an 84 16 UN regulator from Kamstrup Process and connected to a type K-thermocouple (5) placed in a thermowell in the reactor lid. This gave an approximate heating rate of 4.5 °C /min. The reactor outlet was a 3/8″ stainless steel tube in the lid, which led to the condenser (9). The tubing was insulated with foil-faced Rockwool to avoid condensation in the tubing. The condenser was filled with pre-weighed 5 mm glass beads and placed in an ice bath. The condenser was connected to a water trap used to capture ammonia. For each experiment 50 g of polymer mixture was used.

The system was purged with nitrogen for 1–2 min, before each experiment. The reactor was heated to 450 °C where it was held for 30 min before the heating was turned off and nitrogen flow was turned on for 60 min. At all times pressures were kept at ambient pressure. After the pyrolysis the glass beads were washed with dichloromethane (DCM) which was subsequently removed from the oil/DCM mixture using a rotary evaporator (22 °C, 120 rpm) for 60 min. The obtained oil samples were stored in a fridge until analysis.

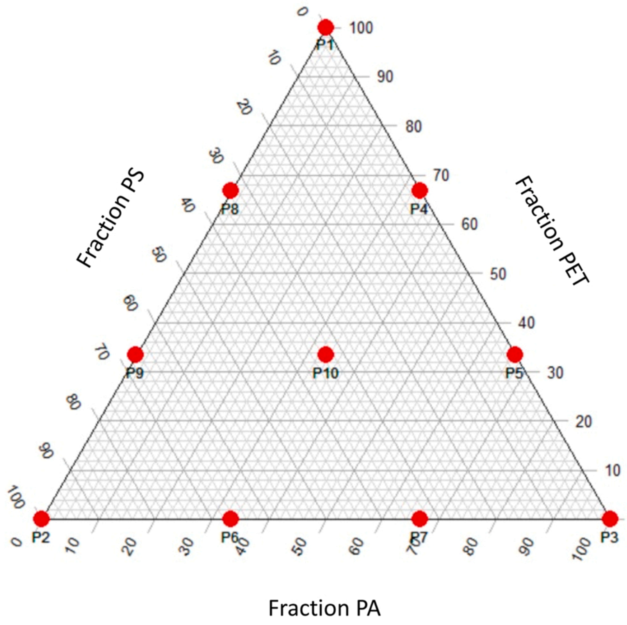

Fig. 1. Sampling points using simplex lattice design. Circles denote experimental compositions.

Table 2
Experimental plan for pyrolysis on a mixture of PP, PE, EVA, PET, PS and PA.

Sample	PP (%)	PE (%)	EVA (%)	PET (%)	PS (%)	PA (%)
P1	70	10	5	15	0	0
P2	70	10	5	0	15	0
P3	70	10	5	0	0	15
P4	70	10	5	10	0	5
P5	70	10	5	5	0	10
P6	70	10	5	0	10	5
P7	70	10	5	0	5	10
P8	70	10	5	10	5	0
P9	70	10	5	5	10	0
P10	70	10	5	5	5	5
P11	70	10	5	15	0	0
P12	70	10	5	0	15	0
P13	70	10	5	0	0	15
P14	70	10	5	10	0	5
P15	70	10	5	5	0	10
P16	70	10	5	0	10	5
P17	70	10	5	0	5	10
P18	70	10	5	10	5	0
P19	70	10	5	5	10	0
P20	70	10	5	5	5	5

The tubing connecting the reactor and condensation vessel and as well as the vessel itself were cleaned using isopropanol. The isopropanol and oil mixtures were transferred to a pre-weighed beaker, which was left for evaporation for at least 72 h, leaving only oil from the condenser and tubing.

2.3. *Analysis*

2.3.1. *Elemental analysis*

The elemental analysis was performed on a 2400 CHNS/O series II system elemental analyzer connected to an AD6 auto-balance controller, both from PerkinElmer. 500 μg oil was used for each analysis and was performed in duplicates.

2.3.2. *GC-MS*

The samples were analyzed on a Clarus® 680 gas chromatograph using an Elite-5 cross bond 5% diphenyl - 95% dimethyl polysiloxane column with cat. #N9316076. Initial conditions were 60 °C for 1 min, before ramping with 15 °C /min to 250 °C and maintained for 10 min.

The mass spectrometer connected was a Clarus® SQ 8. The solvent delay was 2 min, and collection time 2–24 min at 50–600 El+. Each peak was identified using NIST MS Search 2.2 software and assessing the M/Z ratio compared to the suggested compounds to find the best fit.

The samples were prepared by dissolving 4 drops of oil in 4 ml DCM in a test tube. The samples were mixed and filtered before 1.5 ml was transferred to a glass vial for GC-MS for analysis.

2.3.3. *Acid number*

Acid number was measured using a 88 Titrande with electrode #00134718, from Metrohm. A 0.1 M Tetrabutylammonium hydroxide solution was used as titrant. Approximately 1 g was weighed and dissolved in 40 ml of toluene, isopropanol and demineralized water in a volume ratio of 50:49.5:0.5.

2.3.4. *Viscosity*

Viscosity was measured by a Brookfield Model DV-III+ programmable Rheometer with an SC4–18 spindle. 8 ml of samples was placed in a SC4–18 adapter and attached to the rheometer. The maximum rpm was 250, but some samples was measured at lower rpm due to a maximum torque restriction of 80%.

2.3.5. *FT-IR*

FT-IR was performed on a Nicolet iS5 spectrometer attached to an iD7 ATR module from Thermo Scientific. FT-IR was performed with 10 scans and a resolution of 4 in a wavenumber interval of 4000–525 cm^{-1}.

2.4. *Model development*

A linear regression model was developed based on the experimental data. This was done in R using the approach of Lawson & Wilden [27] for fitting mixture models and predicting model coefficients and R^2 values. The models are quadratic Scheffé models given as the following expression:

$$y = \sum_{i=1}^{q} \beta_i x_i + \sum_{i=1}^{q-1} \sum_{j=i+1}^{q} \beta_{ij} x_i x_j + \epsilon$$

3. Results and discussion

In the results and discussion, there is the underlying fact that all the baseline compositon is the same for all experiments, i.e. when discussing a experiment with pure PET this means only PET has been added to the baseline composition. The oils from sample P1 to P10 are shown in

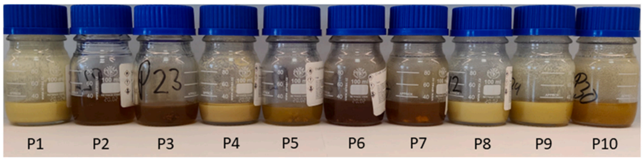

Fig. 3. Picture of oils from sample P1 to P10.

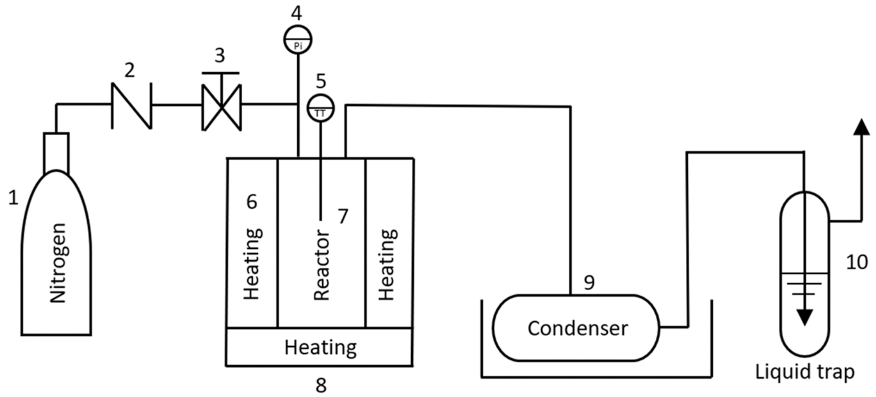

Fig. 2. Principal experimental setup. 1: Nitrogen 2: Check valve 3: Hand-operated valve 4: Pressure indicator 5: Temperature transmitter 6: Heating mantle 7: Reactor 8: Hot plate 9: Condenser in ice bath 10: Liquid water trap.

Fig. 3.

The pyrolysis oil changes appearance according to the feed composition. The oil produced with only PET (P1) is white, while oils from PS (P2) and PA (P3) are dark brown and transparent brown, respectively. When PET is a major part of the feedstock it is observed that the oil remains white, but with increased brownness when mixed with either PS (P8 + P9) and PA (P4 + P5) as well as the mixture of all three (P10). This observation of color changes seems consistent with each polymer producing its own oil and color changes are due to mixing of different colored oils. A solid phase was observed in the pyrolysis oils when PA was present in the feed.

The average mass balances for the experiments are shown in Fig. 4. The span in oil yield, ranging from 77.3 to 90 wt%, is relatively large considering the 15 wt% variation in polymer composition. This can be explained by the presence of PET, which is shown to yield a low amount of oil [7,13]. This is also shown in the results where the experiments containing PET (P1, P4, P8), in general, have lower oil yields, especially compared to the experiments containing PS. The oil yield from experiments with PA is between the yield from PS and PET with 77.3 wt% for PET, 88.2 wt% for PS and 81.4 wt% for PA. This corresponds with the literature, where PET has the smallest oil yield while PS has the highest oil yield [7,17,19]. The variations between repetitions are generally small, showing good repeatability. There are significant differences between the oil yield of the three pure fraction experiments ((P1 + P11), (P2 + P12) and (P3 + P13)). Char content increases with PET content and is lowered as the PA content is increased. Char from PET is caused by combustion due to the PET oxygen content [7,13]. Increased gas formation with PET is due to formation of CO and CO_2.

3.1. Oil composition

The results from elemental analysis are shown in Fig. 5. Elemental analysis shows carbon content around 80% for most samples, except for P2, while hydrogen content is between 6 and 10 wt%. Sulphur and nitrogen content is negligible in all cases. The absence of nitrogen in P3 and P13 is unexpected, as these are based on PA. This indicates that the nitrogen must be part of either the solid particles in the oil or in the gas phase.

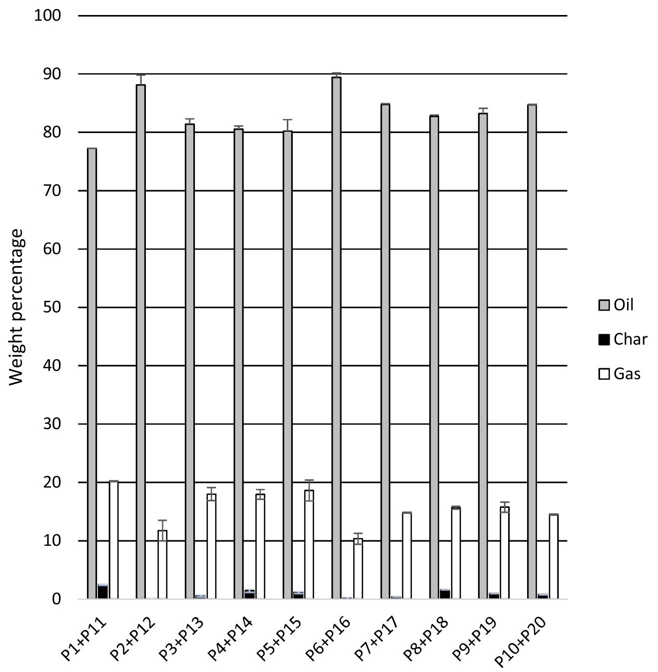

Fig. 4. Average mass balances for all samples with standard deviation. *Gas is calculated by difference.

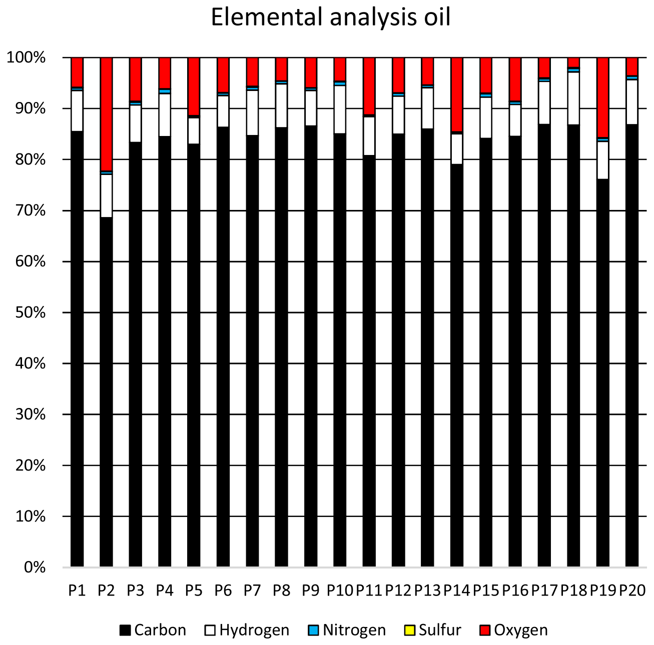

Fig. 5. Elemental analysis of oil. *Oxygen content is calculated by difference.

As can be seen from Fig. 6 the oil contains a large number of components. For each sample the 20–35 largest peak were identified.

The most common compounds are shown in Table 3 with percentage of total peak area in chromatograms, which were calculated assuming that all reponse factors are similar. Most of the compounds are long-chain hydrocarbons as well as 2,4-dimethyl-1-heptene (12.3%–19.5%) which is produced in all cases. 2,4-dimethyl-1-heptene is the main pyrolysis product of PP [13,16] and with 70% of the feedstock consisting of PP this is expected.

The (2,4,6-trimethylcyclohexyl)methanol detected in all samples may be accredited to the co-pyrolysis of PP with oxygen containing compounds, in this case EVA, as shown by Ohja & Vinu [28] when co-pyrolyzing PP and cellulose. With similar concentrations found at all compositions this further indicates that this is produced from the reaction of compounds in the "baseline" composition. With amounts of approx. 2% this appears reasonable as EVA is only present at 5 wt%.

The aromatics, toluene, styrene and 1,1-(1,3-propandiyl)bis-benzene, are only found in samples containing PS, proving that these originate from the PS fraction of the feedstock. This is in line with the findings of Kohli et.al. [29] and the proposed reaction mechanism of Yang et.al. [30].

On the other hand, pentamethylcyclopentane is only found in samples not containing any PS. Benzoic acid is only detected when there is 15% PET in the feed, which shows that 10% PET does not form a significant amount of benzoic acid.

Fig. 7 further expands on these findings by showing the variation in compound class distribution according to the presence of PET, PS and PA.

Generally, the oil consists of hydrocarbons (naphtha, larger hydrocarbons and aromatics) with only a small precense of alcohol and acid. As previously stated, the only acid identified is benzoic acid, which is a product of pyrolysis on PET. Naphta (< C9) is found in all samples in various amounts, most likely the products of PP and PE degradation. Aromatic content increase with increasing amounts of PS but is absent when no PS is added, clearly indicating the relationship between PS and aromatic products.

The hydrocarbon content is shown to increase with increasing PET content while it is lowered as the PS content is increased. Hydrocarbons are generic products and are mainly products from pyrolysis of PE and PP. PE and PP are degraded in the pyrolysis process through a free-

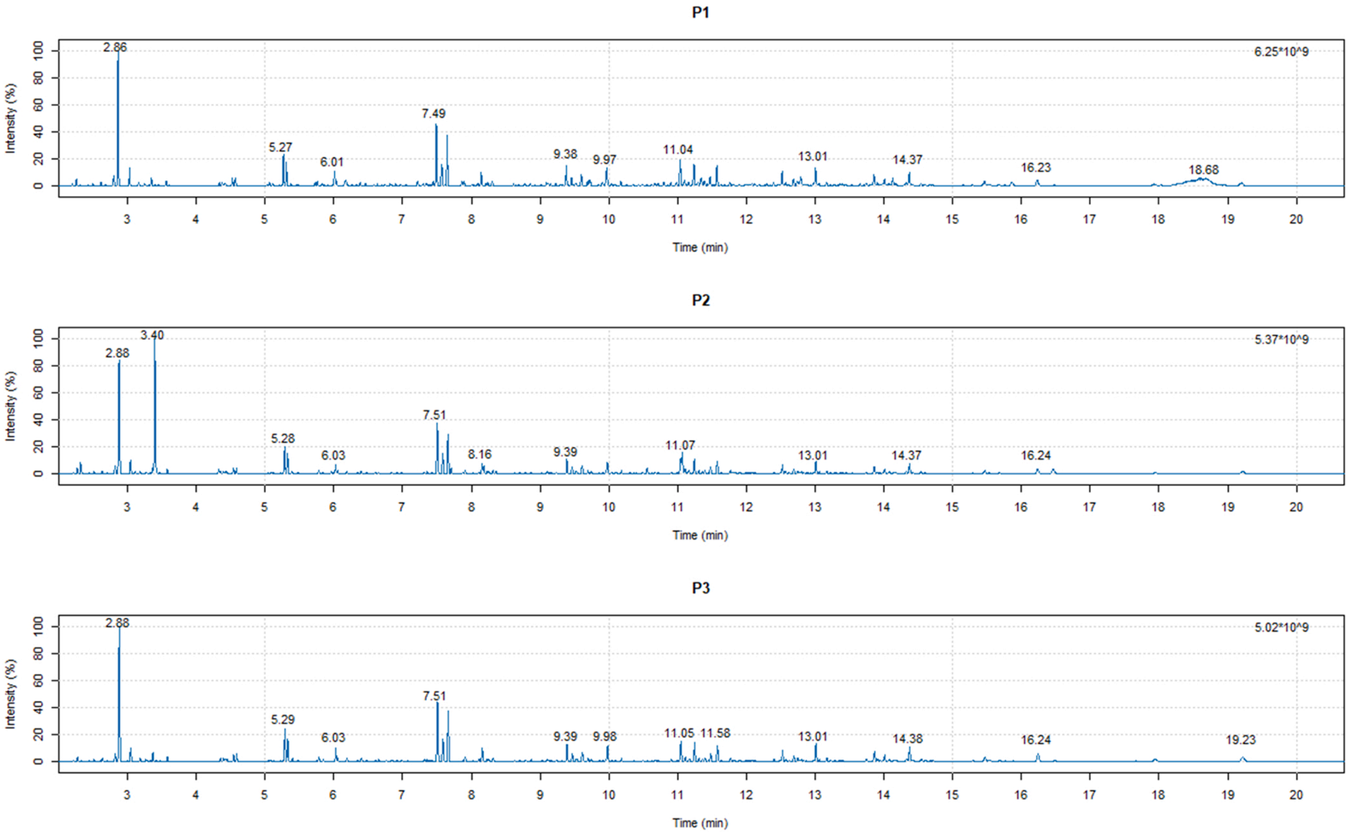

Fig. 6. GC-MS spectra of sample P1, P2 and P3.

Table 3
Average area% of compounds identified in the GC-MS analysis.

Sample **Compound**	**P1 + P11**	**P2 + P12**	**P3 + P13**	**P4 + P14**	**P5 + P15**
Toluene	-	1.7%	-	-	-
Trimethylcyclohexane	4.5%	2.3%	3.5%	5.8%	3.2%
2,4-dimethyl-1-heptene	19.3%	15.3%	18.2%	25.3%	14.6%
Styrene	-	20.5%	-	-	-
Benzoic acid	2.4%	-	-	-	-
Pentamethylcyclopentane	1.0%	-	1.2%	1.3%	1.0%
(2,4,6-trimethylcyclohexyl)methanol	2.4%	1.7%	1.9%	2.6%	1.8%
1,1-(1,3-propandiyl)bis-benzene	-	0.9%	-	-	-
Hydrocarbons, C10-C17	29.4%	26.3%	29.0%	32.4%	30.0%
Hydrocarbons, C18 +	41.1%	31.5%	46.3%	32.7%	49.4%
Sample **Compound**	**P6+P16**	**P7 + P17**	**P8 + P18**	**P9 + P19**	**P10 + P20**
Toluene	1.2%	-	-	1.1%	-
Trimethylcyclohexane	1.7%	1.9%	1.8%	0.7%	2.2%
2,4-dimethyl-1-heptene	14.6%	16.0%	12.3%	15.2%	19.5%
Styrene	14.0%	7.8%	6.4%	14.3%	9.1%
Benzoic acid	-	-	-	-	-
Pentamethylcyclopentane	-	-	-	-	-
(2,4,6-trimethylcyclohexyl)methanol	1.7%	1.8%	1.9%	1.7%	2.0%
1,1-(1,3-propandiyl)bis-benzene	0.8%			0.6%	0.5%
Hydrocarbons, C10-C17	23.4%	31.8%	26.3%	22.8%	28.8%
Hydrocarbons, C18 +	42.7%	40.6%	51.3%	43.5%	37.9%

radical process that includes initiation, propagation and termination combined with random chain scission resulting in generation of a range of different hydrocarbons [29]. The increase in hydrocarbon content with PET can be explained by the lower oil yield as a result of CO and CO_2 generation, and hence the hydrocarbons make up a larger percentage of the oil product.

Using Fig. 7, the main component classes in the oil can be predicted for feed mixtures within the framework of the experimental design. The optimal feed depends on the preferred product, as the compound groups all can be valuable. The use of the triangle is to either pinpoint the expected oil composition or using it to determine whether the plastic waste streams available needs to be modified to reach the preferred oil composition.

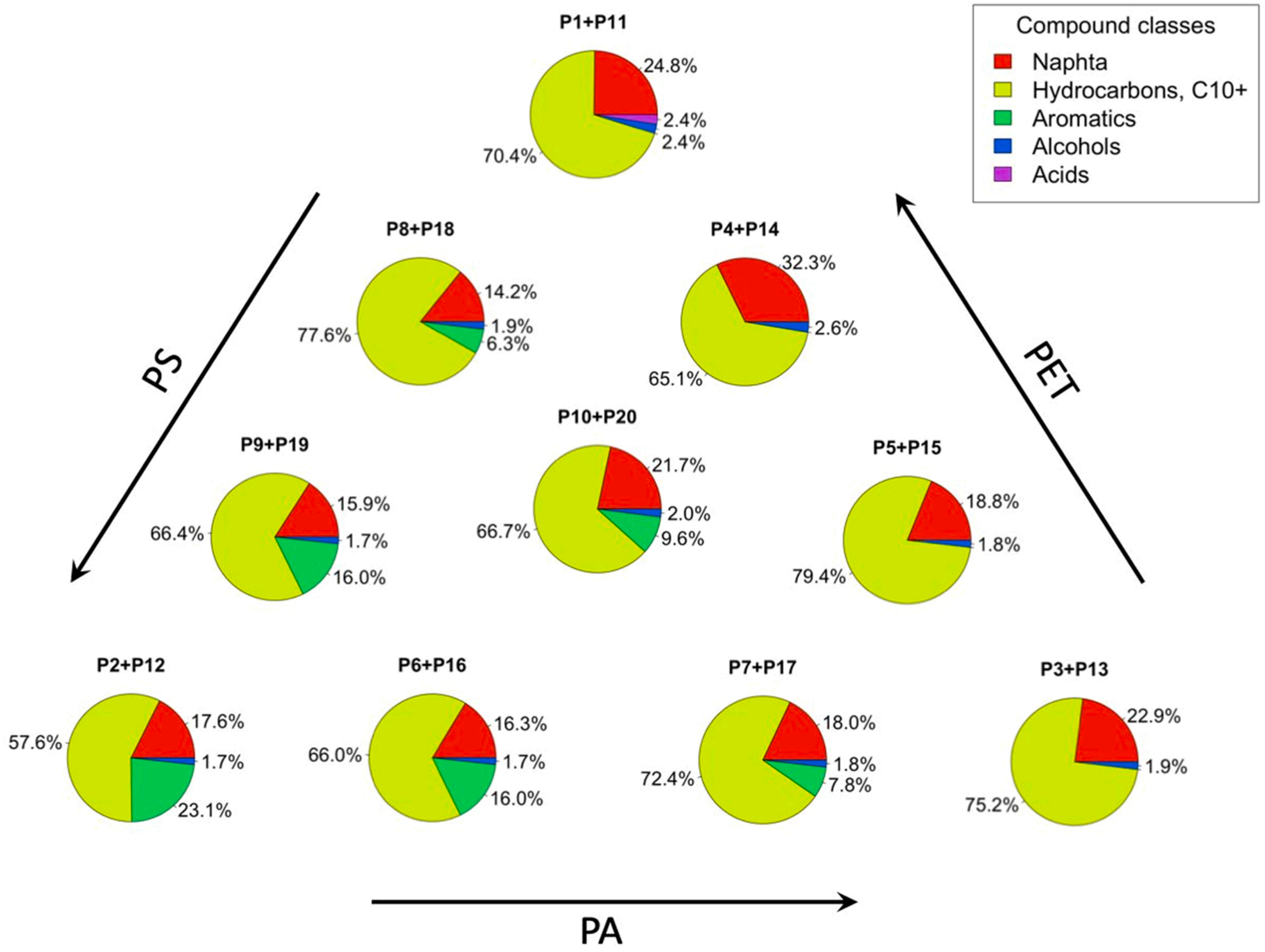

Fig. 7. Compounds divided by compound class arranged by fraction of PS, PET and PA. Each compound identified is divided into compound groups of acid, naphtha, hydrocarbon (C10 +), aromatic hydrocarbons and alcohols. Shown as Average of repetitions.

3.2. Solid phase

A solid phase was formed in the oil when PA was in the feed. This phase was investigated for all samples based on PA except for P26 and P35, which did not contain enough solid phase for analysis. The solid phase was separated from the oil so that the light components in the oil evaporated before analysis. The result of elemental analysis is shown in Fig. 8.

The elemental analysis shows a low carbon content of 55–65% and an oxygen content of 25–30%. This is different from the oil, as the oil contained a larger amount of carbon and lower amounts of oxygen. The nitrogen content varies from 0.7% to 2.9%. This shows that the nitrogen from PA is contained in the solid phase, which is why no nitrogen content was observed in the elemental analysis of the oil. The solid phase was desolved in DCM and analyzed using GC-MS. The main compounds identified were caprolactam and 2-ethoxyethanol. Caprolactam is the PA-6 monomer, which contains nitrogen, while 2-ethoxyethanol contains oxygen, explaining the large amount of oxygen shown in the elemental analysis.

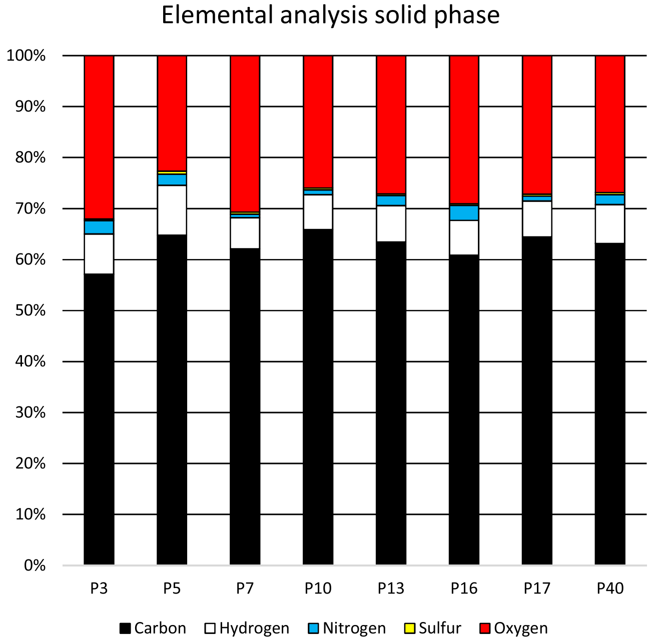

Fig. 8. Elemental analysis solid phase from samples based on PA.

3.3. Oil properties

Results from acid number, viscosity, oil and char yield form the basis for making the regression models for the prediction of responses based on the fraction of PET, PS, and PA. The graphical representation of these models are given in Fig. 9, while coefficients, P-values and corrected R-squared values are shown in Table 4.

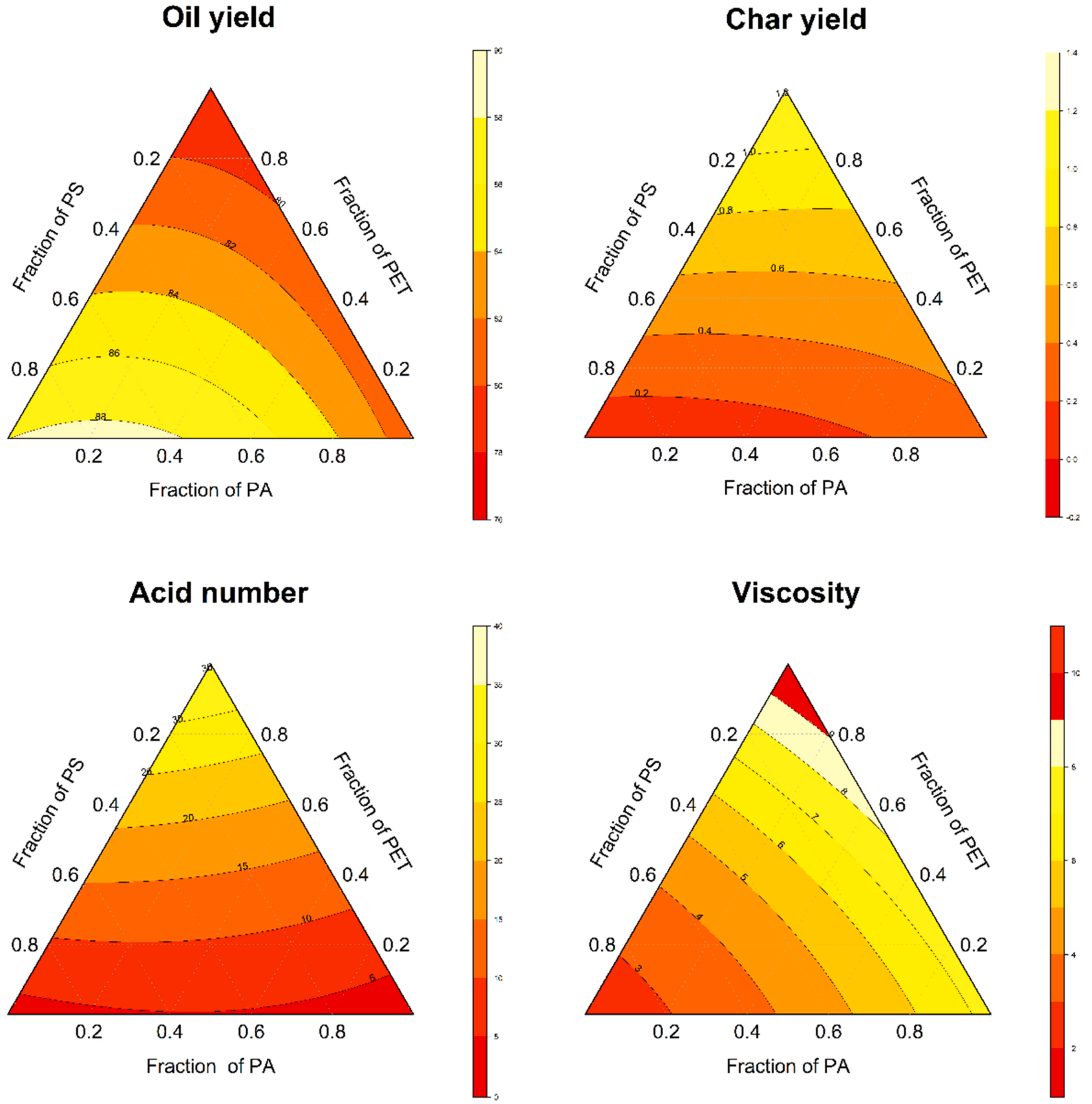

Fig. 9. Contour plots from models for oil yield, char yield, acid number and viscosity.

Table 4
Model coefficients, P-values, and corrected R-squared values for models of oil yield, char yield, acid number and viscosity.

	Oil yield		Char yield		Acid number		Viscosity	
	Coeff.	P-Val.	Coeff.	P-Val.	Coeff.	P-Val.	Coeff.	P-Val.
PET	77.92	$< 2\cdot10^{-16}$	1.22	$6.8\cdot10^{-11}$	35.69	$3.5\cdot10^{-12}$	10.06	$3.8\cdot10^{-10}$
PS	87.98	$< 2\cdot10^{-16}$	0.07	0.34	3.19	0.07	2.47	$2.03\cdot10^{-3}$
PA	80.74	$< 2\cdot10^{-16}$	0.33	$2.94\cdot10^{-4}$	2.39	0.17	7.36	$2.17\cdot10^{-8}$
PS:PET	0.68	0.88	-0.03	0.91	-1.82	0.81	-5.38	0.08
PA:PET	5.14	0.29	-0.51	0.12	-11.57	0.13	-2.87	0.34
PS:PA	12.89	0.02	-0.29	0.37	8.11	0.28	-3.12	0.30
Corr. R^2-val	0.866		0.940		0.962		0.886	

The oil yield increases with the PS content while decreases with the PET content. The oil yield of PA is between the yield of PS and PET. The oil yield varies from 77.3 wt% with a full fraction of PET to 89.9 wt% with a full fraction of PS. This is caused by the content of oxygen in PET, which promotes the formation of both CO, CO_2, and char, thereby lowering the oil yield.

Formation of char is increased with PET content, while PA forms smaller amounts. This is caused by combustion, due to oxygen in PET. Acid number mainly depends on the PET content. It varies from 34 mg KOH/g oil to 1.97 mg KOH/g oil as the PET content is decreased. There does not seem to be any significant difference in the acid number between PS and PA.

Viscosity is mainly increased with the PET fraction, while PA also causes an increase compared to PS. It varies from 2.2 cP with PS to 11.3 cP with PET, which can be ascribed to the formation of wax during pyrolysis of PET.

The model for oil yield explains 87% of the variation showing a good correlation between feed composition and oil yield. All 1st order effect is significant, while the only significant interaction effect is between PA and PS. The coefficients show that PET gives the lowest oil yield, while PS gives the highest oil yield. However, it is shown that oil yield is marginally increased due to interaction of PA and PS. One explanation for this minute increase could be related to the formation of the secondary phase in the samples containing PA which is found to be high in oxygen content. This may suggest that higher amounts of oxygen is remaining in the condensate resulting in a slightly higher oil yield.

The model for char yield explains 94% of the variance, showing a clear correlation between feed composition and char content. PET and PA are significant variables, while PS is not. This is due to the low formation of char during pyrolysis of PS, making it insignificant. No interaction effects were shown to be significant. PET has the largest coefficient at 1.22, while PAś is 0.33, showing that the effect of PET is larger than the effect of PA.

The model for acid number describes 96% of the variance and only depends on PET, as it is the only significant variable. Neither PS nor PA has been shown to form acids during pyrolysis, explaining why only PET has an effect.

The model for viscosity explains 89% of the variation and all polymers are significant. The viscosity is increased most by PET, but also by PA, with coefficients of 10.06 and 7.36 respectively. No interaction effects are shown to be significant.

The models have shown clear correlations between feed composition, yield and oil characteristics, without any major interaction effects identified between the investigated polymer compositions. Hence, the models can be used for the prediction of these parameters if the feed composition is known. The models can also be used to set relatively precise limits for each polymer type, as the models describe the numerical increase in e.g., acid number by a certain increase in PET. This means that a limit for PET can be set, based on the maximum allowed acid number of the oil. Factors to consider when using the model are that they are based on pure polymers, so no additives are affecting the results, and catalysts will affect the relative relationship between the responses investigated [31].

4. Conclusion

Models were created for the prediction of oil yield, char yield, acid number, and viscosity, based on the fraction of PET, PS, and PA. The models showed a decrease in oil yield of 10% when 15% PS was interchanged with PET. PA showed an oil yield in between. Char content, acid number, and viscosity were shown to increase with the content of PET and lowered with the content of PS. PA caused an increase in char yield and viscosity, while it did not affect the acid number. The models R^2-values varied from 0.87 to 0.96, showing that most of the variation in the responses can be explained by the differences in feed composition.

The oil composition is shown to mainly consist of hydrocarbons (C10 +), naphta and aromatics with only a small precense of alcohol and acid. The content of aromatic hydrocarbons is increased by the presence of PS, as this forms styrene and toluene during pyrolysis. The acid content is increased in accordance with the PET content.

CRediT authorship contribution statement

Rasmus Uglebjerg Henneberg: Writing – original draft, Investigation, Formal analysis, Methodology, Visualization. **Rudi Pankratz Nielsen:** Conceptualization, Writing – review & editing, Methodology, Supervision. **Morten Enggrob Simonsen:** Conceptualization, Writing – review & editing, Methodology, Supervision.

Declaration of Competing Interest

The authors declare the following financial interests/personal relationships which may be considered as potential competing interests: Morten Enggrob Simonsen reports a relationship with Quantafuel that includes: equity or stocks. Morten Enggrob Simonsen reports a relationship with European Regional Development Fund that includes: funding grants.

Data Availability

Data will be made available on request.

References

[1] Statista, Annual production of plastics from 1950 to 2020, (2021). https://www.statista.com/statistics/282732/global-production-of-plastics-since-1950/ (Accessed October 7, 2021).

[2] Plastics Europe - Association of Plastic Manufacturers (Organization), Plastics – the Facts 2020, PlasticEurope. (2020) 16.

[3] T. Thiounn, R.C. Smith, Advances and approaches for chemical recycling of plastic waste, J. Polym. Sci. 58 (2020) 1347–1364, https://doi.org/10.1002/pol.20190261.

[4] M.S. Qureshi, A. Oasmaa, H. Pihkola, I. Deviatkin, A. Tenhunen, J. Mannila, H. Minkkinen, M. Pohjakallio, J. Laine-Ylijoki, Pyrolysis of plastic waste: opportunities and challenges, J. Anal. Appl. Pyrolysis 152 (2020), https://doi.org/10.1016/j.jaap.2020.104804.

[5] Z.O.G. Schyns, M.P. Shaver, Mechanical recycling of packaging plastics: a review, Macromol. Rapid Commun. 42 (2021) 1–27, https://doi.org/10.1002/marc.202000415.

[6] Vannessa. Goodship, Introduction to plastics recycling., 2. ed., Smithers Rapra, Shrewsbury, 2007.

[7] S.D. Anuar Sharuddin, F. Abnisa, W.M.A. Wan Daud, M.K. Aroua, A review on pyrolysis of plastic wastes, Energy Convers. Manag. 115 (2016) 308–326, https://doi.org/10.1016/j.enconman.2016.02.037.

[8] M. Roosen, N. Mys, M. Kusenberg, P. Billen, A. Dumoulin, J. Dewulf, K.M. Van Geem, K. Ragaert, S. De Meester, Detailed analysis of the composition of selected plastic packaging waste products and its implications for mechanical and thermochemical recycling, Environ. Sci. Technol. 54 (2020) 13282–13293, https://doi.org/10.1021/acs.est.0c03371.

[9] B. Ruj, V. Pandey, P. Jash, V.K. Srivastava, Sorting of plastic waste for effective recycling, Int. J. Appl. Sci. Eng. Res. 4 (2015) 564–571.

[10] K. Kaiser, M. Schmid, M. Schlummer, Recycling of polymer-based multilayer packaging: a review, Recycling 3 (2018), https://doi.org/10.3390/recycling3010001.

[11] K. Murata, K. Sato, Y. Sakata, Effect of pressure on thermal degradation of polyethylene, J. Anal. Appl. Pyrolysis 71 (2004) 569–589, https://doi.org/10.1016/j.jaap.2003.08.010.

[12] M.S. Abbas-Abadi, M.N. Haghighi, H. Yeganeh, A.G. McDonald, Evaluation of pyrolysis process parameters on polypropylene degradation products, J. Anal. Appl. Pyrolysis 109 (2014) 272–277, https://doi.org/10.1016/j.jaap.2014.05.023.

[13] S.M. Fakhrhoseini, M. Dastanian, Predicting pyrolysis products of PE, PP, and PET using NRTL activity coefficient model, J. Chem. (2013), https://doi.org/10.1155/2013/487676.

[14] I. Ahmad, M. Ismail Khan, H. Khan, M. Ishaq, R. Tariq, K. Gul, W. Ahmad, Pyrolysis study of polypropylene and polyethylene into premium oil products, Int. J. Green. Energy 12 (2015) 663–671, https://doi.org/10.1080/15435075.2014.880146.

[15] S. Kumar, R.K. Singh, Recovery of hydrocarbon liquid from waste high density polyethylene by thermal pyrolysis, Braz. J. Chem. Eng. 28 (2011) 659–667, https://doi.org/10.1590/S0104-66322011000400011.

[16] A. Demirbas, Pyrolysis of municipal plastic wastes for recovery of gasoline-range hydrocarbons, J. Anal. Appl. Pyrolysis 72 (2004) 97–102, https://doi.org/10.1016/j.jaap.2004.03.001.

[17] J.A. Onwudili, N. Insura, P.T. Williams, Composition of products from the pyrolysis of polyethylene and polystyrene in a closed batch reactor: Effects of temperature and residence time, J. Anal. Appl. Pyrolysis 86 (2009) 293–303, https://doi.org/10.1016/j.jaap.2009.07.008.

[18] D.W. Zeng, M. Born, K. Wambach, Pyrolysis of EVA and its application in recycling of photovoltaic modules, J. Environ. Sci. 16 (2004) 889–893.

[19] A.M. Pannase, R.K. Singh, B. Ruj, P. Gupta, Decomposition of polyamide via slow pyrolysis: Effect of heating rate and operating temperature on product yield and composition, J. Anal. Appl. Pyrolysis 151 (2020), 104886, https://doi.org/10.1016/J.JAAP.2020.104886.

[20] P.T. Williams, E. Slaney, Analysis of products from the pyrolysis and liquefaction of single plastics and waste plastic mixtures, Resour., Conserv. Recycl. 51 (2007) 754–769, https://doi.org/10.1016/j.resconrec.2006.12.002.

[21] A.A. Casazza, E. Spennati, A. Converti, G. Busca, Study on the thermal decomposition of plastic residues, Chem. Eng. Trans. 74 (2019) 1141–1146, https://doi.org/10.3303/CET1974191.

[22] Y. Yoshida, K. Kono, A. Harada, S. Toyota, M. Watanabe, K. Iwasaki, Toxicity of pyrolysis products of thermal-resistant plastics including polyamide and polyester, Nippon Eiseigaku Zasshi. Jpn. J. Hyg. 33 (1978) 450–458, https://doi.org/10.1265/jjh.33.450.

[23] M.M. Hirschler, M.M. Morgan, Thermal Decomposition of Polymers, in: P. J. DiNenno (Ed.), Chemistry of Materials, NFPA, Quincy,MA, 2008, pp. 3495–3508.

[24] S. Budsaereechai, A.J. Hunt, Y. Ngernyen, Catalytic pyrolysis of plastic waste for the production of liquid fuels for engines, RSC Adv. 9 (2019) 5844–5857, https://doi.org/10.1039/c8ra10058f.

[25] S.V. Levchik, E.D. Weil, M. Lewin, Thermal decomposition of aliphatic nylons, Polym. Int. 48 (1999) 532–557, https://doi.org/10.1002/(sici)1097-0126(199907)48:7<532::aid-pi214>3.0.co;2-r.

[26] M.L. Marfn, A. Jtm~nez, J. Lrpez, J. Vilaplana, Thermal degradation of ethylene (vinyl acetate) Kinetic analysis of thermogravimetric data 9 I, J. Therm. Anal. 47 (1996) 247–258.

[27] J. Lawson, C. Willden, Mixture experiments in R using mixexp, J. Stat. Softw. 72 (2) (2016) 1–20, https://doi.10.18637/jss.v072.c02.

[28] D.K. Ojha, R. Vinu, Fast co-pyrolysis of cellulose and polypropylene using Py-GC/MS and Py-FT-IR, RSC Adv. 5 (2015) 66861, https://doi.10.1039/c5ra10820a.

[29] K. Kohli , S.R. Chandrasekaran , R. Prajapati , B. Kunwar , S. Al-Salem , B.R. Moser , B.K. Sharma , Pyrolytic Depolymerisation Mechanisms for Post-Comsumer Plactic Wastes energies, 15, 2022, 8821–8845. https://doi.org/10.3390/en15238821.

[30] M. Yang, Y. Shibasaki, Mechanisms of thermal degradation of polystryrene, polymethacrylonitrile, and their copolymers on flash pyrolysis, J. Polym. Sci. Part A Polym. Chem. 36 (1998) 2315–2330.

[31] L. Quesada, M.C. de Hoces, M.A. Martín-Lara, G. Luzón, G. Blázquez, Performance of different catalysts for the in situ cracking of the oil-waxes obtained by the pyrolysis of polyethylene filmwaste, Sustain. (Switz.) 12 (2020) 1–15, https://doi.org/10.3390/su12135482.